A 1-ml aliquot of the psoralen-treated stock (1 mg/ml) was diluted in 6 ml of PBS. Two milliliters of the diluted stock were added to the Ribi adjuvant system (Ribi ImmunoChem Research), in accordance with the manufacturer's specifications, and 0.2 ml were administered into the peritoneum. Mice were given booster inoculations on days 21 and 48.
17. M. E. Andrew, B. E. Coupar, D. B. Boyle, *Immunol. Cell Biol.* **67**, 331 (1989).
18. We thank L. H. Miller for insight and support. We thank R. Schwartz for providing congenic mice; F. A. Neva, S. Kumar, and D. Rawlings for critically reviewing the manuscript; and J. A. Bersofsky and J. Sadoff for useful discussions. This investigation received financial support from the United Nations Development Programme–World Bank–World Health Organization Special Programme for Research and Training in Tropical Diseases.

19 October 1990; accepted 15 February 1991

Two- Rather Than Three-Dimensional Representation of Saccades in Monkey Superior Colliculus

A. JOHN VAN OPSTAL,* KLAUS HEPP, BERNHARD J. M. HESS, DOMINIK STRAUMANN, VOLKER HENN

Saccades are controlled by neurons in the brainstem reticular formation that receive input from the superior colliculus and cortex. Recently two quantitative models have been proposed for the role of the colliculus in the generation of three-dimensional eye movements. In order to test these models, three-dimensional eye movements were measured in the alert monkey to investigate whether the saccadic motor map of the superior colliculus is two-dimensional, representing retinal target vectors, or three-dimensional, representing three-dimensional motor error for the rotation of the eye. Electrical stimulation of the superior colliculus produced two-dimensional, not three-dimensional, eye movements. It is therefore concluded that the collicular motor map is two-dimensional.

THE MONKEY SUPERIOR COLLICULUS (SC) is a brainstem structure that is important in the generation of saccadic eye movements (*1*). Electrical stimulation of the SC produces saccades with short latencies at low stimulation thresholds. Saccade amplitude and direction depend predominantly on the site of stimulation (*2, 3*). Cells in the deeper layers of the SC burst vigorously for saccades that are directed into their movement field (the range of saccade vectors for which a particular SC cell is activated), and the neural activity related to movement is tightly coupled to saccade onset (*1, 4*). Furthermore, the SC provides an important input to the reticular formation, where the burst generator for all rapid eye movements is situated (*5, 6*). Whereas ablation of the SC (*7, 8*) causes only minor permanent deficits in saccadic performance, small local injections of either muscimol or lidocaine (*9*), which inhibit neural activity, cause profound deficits for saccades directed into the affected movement field. Parallel pathways, presumably incorporating the frontal eye field (FEF), may be able to compensate for most of the deficits after ablation of the SC (*7*).

So far, researchers have investigated the function of the SC by measuring eye movements in two dimensions (horizontal and vertical). Recently, however, theoretical studies have shown that a complete description of the rotational kinematics of eye movements must be in three dimensions, that is, it must include torsion (*10, 11*). There are two ways of describing the kinematics of saccades. One description is a trajectory; eye position is described by a virtual rotation from a head-fixed reference position (primary position). Experimental evidence shows that all virtual rotation axes describing eye positions lie in a single plane [Listing's law (*12*)], which is defined as Listing's plane (Fig. 1) if the head is upright and stationary. The other description uses the rotation of the eye from the starting position of the saccade to the instantaneous position. It has been shown experimentally that in this description saccades have fixed angular velocity axes that are not confined to a plane (*13*) and therefore require a three-dimensional (3-D) parameter space. These two descriptions are equivalent and are a consequence of the noncommutativity of rotations in 3-D space (*10, 11*).

We have investigated the neural implementation of Listing's law. Listing's law may be implemented upstream from the motor SC [the quaternion model (*11*)]. The axis, when the eye moves from initial position $\mathbf{r}_A$ to final position $\mathbf{r}_B$, both in Listing's plane (Fig. 1), is thought to be coded in the motor colliculus as the rotation vector (*10, 14, 15*):

$$\mathbf{r}_{AB} \approx \mathbf{r}_B - \mathbf{r}_A + \mathbf{r}_A \times \mathbf{r}_B \qquad (1)$$

where $\times$ denotes the vector outer product (*10, 11*). In this model, the collicular vector $\mathbf{r}_{AB}$, the direction of which is the angular velocity axis of an eye rotation, will, in general, be tilted out of Listing's plane because its torsional component, $r^x_{AB} = (\mathbf{r}_A \times \mathbf{r}_B)^x$, is nonzero whenever $\mathbf{r}_A$ and $\mathbf{r}_B$ are nonparallel rotation vectors (*13*).

A corollary of Eq. 1 is that electrical stimulation will, in general, yield saccades that bring the eye out of Listing's plane (*11*) in a specific way: the torsional component of the eye, achieved after stimulation, is determined by

$$r^x_S \approx \|\mathbf{r}_{AB}\| \cdot r^{\perp} \qquad (2)$$

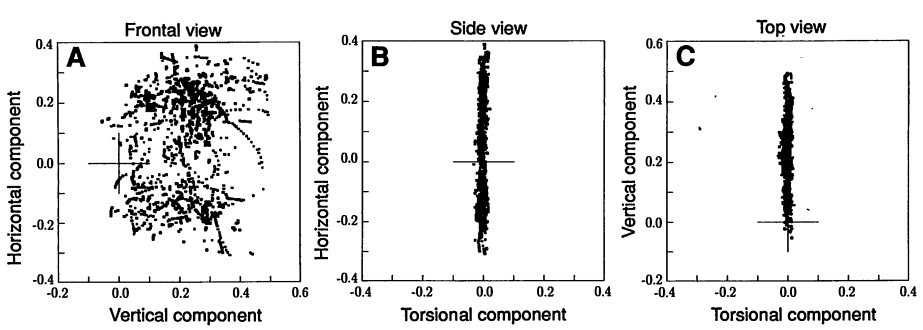

Fig. 1. Listing's law for eye position of visually evoked eye movements. Eye positions (*15*) were sampled at regular intervals during and between saccades in the light (1575 data points) with the head pitched downward by 15°. All eye positions lie in a well-defined plane with zero torsion. Typical standard deviation in the torsional direction was less than 1°. The plane is perpendicular to the torsional direction, thus defining the direction of primary position (cross mark). Data from monkey Ca. (**A**) Frontal (horizontal-vertical) view of Listing's plane. The center of the oculomotor range is, for this monkey, downward from primary position. (**B**) Side view of Listing's plane along the interaural line. (**C**) Top view of Listing's plane along the vertical axis. Units for both figures are the following: a rotation vector component of 0.1 corresponds approximately to $\rho = 10°$ according to the formula $\mathbf{r} = \tan(\rho/2) \cdot \mathbf{n}$ (*14, 15*).

A. J. van Opstal, B. J. M. Hess, D. Straumann, V. Henn, Neurology Department, University Hospital, CH-8091 Zürich, Switzerland.
K. Hepp, Physics Department, Eidgenössische Technische Hochschule, CH-8093 Zürich, Switzerland.

*To whom correspondence should be addressed, at the Department of Medical Physics and Biophysics, University of Nijmegen, Geert Grooteplein Noord 21, 6525 EZ Nijmegen, The Netherlands.

where $\mathbf{r}_{AB}$ is given by Eq. 1 and $r^{\perp}$ is the component of the onset position vector, $\mathbf{r}_{on}$, that is orthogonal to the rotation axis $\mathbf{r}_{AB}$ (*16*).

A second consequence of this model is that collicular movement fields are 3-D even for visually evoked saccades. One should therefore find that the majority of cells have their movement field center outside Listing's plane. Such cells will fire optimally for saccades having a rotational axis with a specific torsional component, and their firing rate should thus depend in a systematic way on saccade onset position.

On the other hand, the SC may be conceived as a two-dimensional (2-D) oculocentric motor map (*2*) that elicits horizontal and vertical components of saccades corresponding to the desired eye displacement (*10*), $\mathbf{d}_{AB}$, from Listing position $\mathbf{r}_A$ to $\mathbf{r}_B$: $\mathbf{d}_{AB} = \mathbf{r}_B - \mathbf{r}_A$ (the vector model). Thus, the torsional component of the angular velocity vector, if needed by the eye-muscle system, is determined downstream of the SC, for example, in an eye position–dependent feedback loop (*10*). In this model, the centers of collicular movement fields are all in Listing's plane (*17*), and no deviation of Listing's law is expected after saccades elicited by electrical stimulation: $\mathbf{r}_S = \mathbf{d}_{AB} + \mathbf{r}_{on}$.

We have tested the predictions of these two models by measuring eye position in three dimensions in three alert rhesus monkeys with an implanted dual scleral search coil (*18, 19*). We electrically stimulated the deeper layers of the SC (110 sites in six colliculi; current strengths between 10 and 100 μA) at locations where neural activity related to movement had been recorded earlier, while letting the monkey look around; we thereby obtained a large range of initial eye positions in Listing's plane.

Microstimulation at a typical site of the right SC of monkey Ca yielded saccade trajectories in the horizontal-vertical and horizontal-torsional plane (Fig. 2, A and B). We examined the amount of eye torsion after electrically evoked saccades as a function of $\mathbf{r}^{\perp}$ (Eq. 2) (Fig. 2C). A least squares regression fit for the data points (slope, -0.0037 ± 0.001) is much closer to the prediction (slope, 0.0) of the vector model than that of the quaternion model. The results for all stimulation sites are presented in Fig. 2D. If the quaternion model applied to our data, the values would be scattered around the line with slope 1.0 (line *Q*). Instead, the data are much closer to the horizontal axis, although a weak relation emerges, especially for large-amplitude sites. The results obtained for monkeys Br and Ce are similar to those for monkey Ca. The slight slopes that we found might partly be due to nonlinearities of the eyeball–eye muscle system when the eye reaches the limits of its motor range.

We conclude that Listing's law is implemented downstream of the SC on the basis of experimental data with electrical microstimulation. Our interpretation is further supported by the results of single unit analysis in the SC (*17*). Because a parallel pathway that bypasses the SC is known to exist, by which the FEF can send its signals directly to the reticular formation (*7*), Listing's law may be implemented upstream from the SC. As Listing's law is preserved after collicular stimulation (Fig. 2), this possibility would require the bypass pathway to provide on-line torsional error. Since local inactivation of the SC reduces the dynamics of saccades into the affected movement field (*9*), which suggests that this parallel pathway may in fact be normally ineffective, the possibility of such fast and accurate on-line error feedback of eye torsion is unlikely. Also, a bilateral chemical inactivation of neuron populations in the SC, which was large enough to drastically reduce the frequency and amplitude of visually elicited saccades, did not lead to a deterioration of Listing's plane for the remaining spontaneous eye movements and did not abolish rapid phases of the vestibulo-ocular reflex in three dimensions (*20*).

These results are different from those obtained from neurons in the rostral interstitial nucleus of the medial longitudinal fasciculus (riMLF) in the midbrain, the structure that directly controls the motoneurons that generate vertical and torsional rapid eye movement components. A bilateral riMLF lesion leads to the permanent loss of all rapid eye movements with a vertical or torsional component; this result functionally localizes the riMLF between the SC and the extraocular motoneurons (*6*). Analysis of unit activity in the riMLF reveals that many neurons code torsional movement components: unilateral inactivation leads to torsional deficits (*6*), and electrical stimulation always induces eye movements with a torsional component (*21*).

We postulate that Listing's law for visually evoked saccades is implemented downstream of the SC. Like the visual map in the superficial layers, the motor map in the deeper layers of the SC is organized in oculocentric coordinates. This 2-D organization greatly simplifies multisensory coordination, such as the generation of saccades to auditory targets (*22*) or the coordination of eye and head (*23*) or eye and arm (*24*).

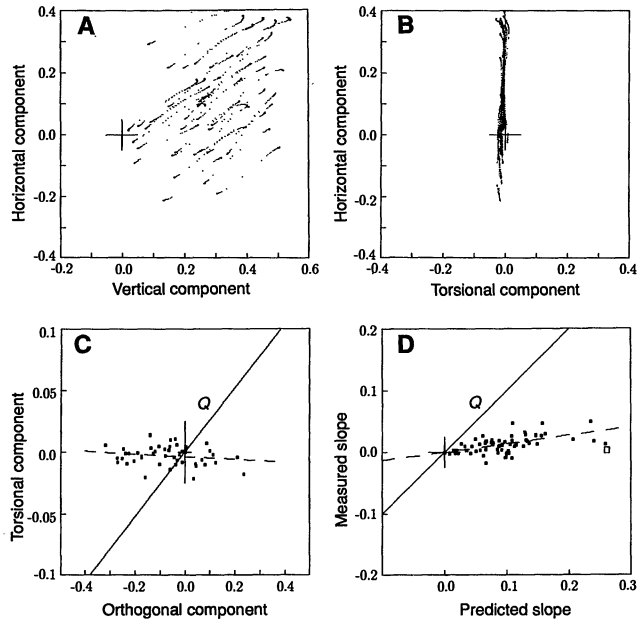

Fig. 2. Results of electrical stimulation in deeper layers of right SC. Data from monkey Ca. (**A**) Saccade trajectories in the *yz* plane as a result of electrical microstimulation at site ca1542 (50-μA cathodal pulses; train duration, 70 ms; pulse width, 0.25 ms; 330 Hz). Starting positions of the eye were scattered widely within the oculomotor range. Saccades were directed leftward and downward. Mean amplitude equals 29.3°. (**B**) Same data as in (A) in side view. Saccades remain in Listing's plane. (**C**) Quantitative test of the prediction of the quaternion model (Eq. 2) and the vector model for collicular coding of saccades. Data from (A) and (B). The continuous line (Q) represents the prediction of the quaternion model (slope $\|\mathbf{r}_{AB}\| = 0.261$), whereas the dotted line is the fitted regression line through the data points ($r_S^{\times} = -0.0113 - 0.0037 \cdot r^{\perp}$; SD of fitted slope: $\sigma_s = 0.001$; $n = 47$). Note the differences in scale for ordinate and abscissa. (**D**) Result of analysis, as in (C), for all stimulation sites in monkey Ca. [□, data from (C)]. Predicted slope based on the quaternion model (given by $\|\mathbf{r}_{AB}\|$). Measured slopes (α) from data based on regression line analysis. Linear regression yields $\alpha = -0.0001 + 0.102 \cdot \|\mathbf{r}_{AB}\|$ ($\sigma_s = 0.006$; $n = 63$), which is close to $\alpha = 0.0$. Similar results were obtained for monkey Br: $\alpha = 0.0214 + 0.161 \cdot \|\mathbf{r}_{AB}\|$ ($\sigma_s = 0.02$; $n = 31$), and monkey Ce: $\alpha = -0.0121 + 0.227 \cdot \|\mathbf{r}_{AB}\|$ ($\sigma_s = 0.007$; $n = 46$).

REFERENCES AND NOTES

1. P. H. Schiller and F. Koerner, *J. Neurophysiol.* **34**, 920 (1971); P. H. Schiller and M. Stryker, *ibid.* **35**, 915 (1972); R. H. Wurtz and M. E. Goldberg, *ibid.*, p. 575.
2. D. A. Robinson, *Vision Res.* **12**, 1795 (1972).
3. A. J. van Opstal, J. A. M. van Gisbergen, A. C. Smit, *Exp. Brain Res.* **79**, 299 (1990).
4. D. L. Sparks and L. E. Mays, *Brain Res.* **190**, 39 (1980); D. L. Sparks, *ibid.* **156**, 1 (1978).
5. M. S. Raybourn and E. L. Keller, *J. Neurophysiol.* **40**, 861 (1977).
6. K. Hepp, V. Henn, T. Vilis, B. Cohen, in *The Neurobiology of Saccadic Eye Movements*, R. H. Wurtz and M. E. Goldberg, Eds. (Elsevier, Amsterdam, 1989), pp. 105–212.

7. P. H. Schiller, S. D. True, J. L. Conway, *J. Neurophysiol.* **44**, 1175 (1980).
8. J. E. Albano, M. Mishkin, L. E. Westbrook, R. H. Wurtz, *ibid.* **48**, 338 (1982).
9. O. Hikosaka and R. H. Wurtz, *ibid.* **53**, 266 (1985); *Exp. Brain Res.* **61**, 531 (1986); C. Lee, W. H. Rohrer, D. L. Sparks, *Nature* **332**, 357 (1988).
10. K. Hepp, *Commun. Math. Phys.* **132**, 285 (1990).
11. D. B. Tweed and T. Vilis, *J. Neurophysiol.* **58**, 832 (1987); *Neural Networks* **3**, 75 (1990).
12. H. von Helmholtz, *Handbuch der Physiologischen Optik* (Voss, Hamburg, 1896).
13. D. B. Tweed and T. Vilis, *Ann. N.Y. Acad. Sci.* **545**, 128 (1988).
14. W. Haustein, *Biol. Cybern.* **60**, 411 (1989).
15. Three-dimensional eye positions are expressed as rotation vectors (*10, 14*): $\mathbf{r} = \tan(\rho/2) \cdot \mathbf{n}$, where $\mathbf{n}$ is the normalized axis about which the eye has to rotate to go from primary position to the current eye position and ρ is the amount of rotation about $\mathbf{n}$. This notation is fully equivalent to the quaternion representation (*11, 13*). We have adopted a right-handed coordinate system: torsion is the component of $\mathbf{r}$ along the forward-pointing x axis (right ear down rotation, positive), vertical position along the leftward-pointing y axis (downward, positive), and horizontal position along the upward-pointing z axis (leftward, positive). As an example, a position 20° to the left of primary position $[(x,y,z) = (0,0,0)]$ is represented by the coordinates $(x,y,z) \doteq (0,0,0.176)$. All mathematical expressions in Eqs. 1 and 2 are evaluated up to third-order corrections in the angle ρ, an error that is beyond experimental resolution.
16. Equation 2 follows from Eq. 1 if one substitutes $\mathbf{r}_B$ by $\mathbf{r}_{AB}$ (the stimulation-induced rotation) and $\mathbf{r}_A$ by $\mathbf{r}_{on}$ (the initial eye position) and calculates the torsional component. We use the fact that both $\mathbf{r}_{on}$ (Fig. 1) and $\mathbf{r}_{AB}$ (not shown) lie in Listing's plane.
17. The results of our analysis are consistent with two-dimensional movement fields: K. Hepp, A. J. van Opstal, B. J. M. Hess, D. Straumann, V. Henn, *Soc. Neurosci. Abstr.* **16**, 1084 (1990).
18. D. A. Robinson, *IEEE Trans. Biomed. Eng.* **10**, 137 (1963); L. Ferman, H. Collewijn, T. C. Jansen, A. V. van den Berg, *Vision Res.* **27**, 811 (1987).
19. B. J. M. Hess, *Vision Res.* **30**, 597 (1990).
20. A. J. van Opstal, V. Henn, B. J. M. Hess, D. Straumann, K. Hepp, *Soc. Neurosci. Abstr.* **16**, 1084 (1990).
21. V. Henn, D. Straumann, B. J. M. Hess, A. J. van Opstal, K. Hepp, in *Vestibular and Brain Stem Control of Eye, Head and Body Movements*, H. Shimazu and Y. Shinoda, Eds. (Springer, Heidelberg, Germany, 1991).
22. M. F. Jay and D. L. Sparks, *J. Neurophysiol.* **57**, 35 (1987).
23. D. Tweed and T. Vilis, *Soc. Neurosci. Abstr.* **14**, 958 (1988); D. Straumann, K. Hepp, Th. Haslwanter, A. J. van Opstal, *Eur. J. Neurosci. Suppl.* **3**, 163 (1990).
24. D. Straumann, T. Haslwanter, M. C. Hepp-Reymond, K. Hepp, *Exp. Brain Res.*, in press.
25. We thank V. Furrer-Isoviita and M. Dürsteler for technical assistance. Supported by the European Strategic Programme for Research and Development in Information Technology (Mucom 3149 and SNF 3199-025239) (A.J.V.O.); SNF 28008.89 (B.J.M.H. and D.S.) and EMDO-Stiftung Zürich (D.S.).

9 October 1990; accepted 11 March 1991

Neuronal Activity in Narcolepsy: Identification of Cataplexy-Related Cells in the Medial Medulla

JEROME M. SIEGEL,* ROBERT NIENHUIS, HEIDI M. FAHRINGER, RICHARD PAUL, PRIYATTAM SHIROMANI, WILLIAM C. DEMENT, EMMANUEL MIGNOT, CHARLES CHIU

Narcolepsy is a neurological disorder characterized by sleepiness and episodes of cataplexy. Cataplexy is an abrupt loss of muscle tone, most often triggered by sudden, strong emotions. A subset of cells in the medial medulla of the narcoleptic dog discharged at high rates only in cataplexy and rapid eye movement (REM) sleep. These cells were noncholinergic and were localized to ventromedial and caudal portions of the nucleus magnocellularis. The localization and discharge pattern of these cells indicate that cataplexy results from a triggering in waking of the neurons responsible for the suppression of muscle tone in REM sleep. However, most medullary cells were inactive during cataplexy but were active during REM sleep. These data demonstrate that cataplexy is a distinct behavioral state, differing from other sleep and waking states in its pattern of brainstem neuronal activity.

THE NARCOLEPTIC DOG EXHIBITS most of the symptoms of human narcolepsy. It has episodes of cataplexy, the loss of antigravity muscle tone triggered by emotional excitement. It also has periods of REM sleep just after sleep onset and increased sleepiness, as in the human condition (*1*). Canine and human cataplexy have similar pharmacological responses; both are exacerbated by α_1 noradrenergic blockers (*2*) and improved by amphetamine, methylphenidate, and related drugs and by antidepressants (*3–5*). Both human and canine narcolepsy are genetically determined (*4, 6*).

It has been hypothesized that narcolepsy is a disease of REM sleep regulation (*7*). Accordingly, the cataplexy and sleep paralysis of narcolepsy represent a triggering during waking of mechanisms that normally suppress muscle tone during REM sleep. Similarly, the hypnagogic hallucinations of narcolepsy result from a release of the dream imagery of REM sleep into waking, and the REM sleep periods at sleep onset result from a loss of mechanisms that normally delay this state until after non-REM sleep. With the narcoleptic dog, one can investigate this hypothesis at the cellular level.

The suppression of muscle tone during REM sleep requires the integrity of the dorsolateral pons (*8*) and the medial medulla (*9*). Chemical stimulation studies have identified two distinct medullary regions that mediate muscle tone suppression: a rostroventromedial region corresponding to the ventral and caudal portions of the nucleus magnocellularis (NMC) and a caudomedial region corresponding to the nucleus paramedianus (*10*). A cell type within the medial medulla and dorsolateral pons has a high discharge rate during REM sleep and a low discharge rate during both active and quiet waking (*11–14*). This cell type is absent in adjacent pontine and medullary regions that are not required for atonia (*15, 16*). If cataplexy represents an abnormal activation of the atonia mechanism of REM sleep, then there should be a population of cells that is maximally active during both REM sleep and cataplexy in these regions. To search for these cells, we recorded the unit activity in the medial medulla of the narcoleptic dog during sleep-waking states and during cataplectic attacks.

Four narcoleptic dogs (Doberman-Labrador crossbreeds) were implanted through the interparietal bone with modified microdrives of the type that we have used in the freely moving cat (*16*). Each drive propelled two bundles of seven 32-μm microwires, and each animal had two microdrives. The microdrives passed through the transverse sinus, necessitating careful hemostasis during surgery, and then through the cerebellum and fourth ventricle, with the microwires projecting into the medulla.

J. M. Siegel, R. Nienhuis, H. M. Fahringer, R. Paul, C. Chiu, Neurobiology Research, Veterans Affairs Medical Center, Sepulveda, CA 91343, and Department of Psychiatry and Brain Research Institute, UCLA School of Medicine, Los Angeles, CA 90024.
P. Shiromani, Department of Psychiatry, San Diego Veterans Affairs Medical Center, and University of California, La Jolla, CA 92093.
W. C. Dement and E. Mignot, Department of Psychiatry, Stanford University School of Medicine, Palo Alto, CA 94305.

*To whom correspondence should be addressed.

Table 1. Discharge rates (spikes per second) of medial medullary cells in sleep-wake states and cataplexy.

Cell type	Quiet waking	Active waking	Cataplexy	REM	Non-REM	*n*
Cataplexy-off	8.8	20.8	5.4	17.9	6.9	52
Cataplexy-on	9.2	6.7	16.4	19.5	4.6	10
Other	13.1	15.8	13.9	23.3	12.4	24